J. Pharm. Pharmac., 1969, **21**, *Suppl.*, 30 S–39 S *Received May* 1, 1969

The effect of particle shape on powder properties

K. RIDGWAY AND R. RUPP

*The Department of Pharmaceutics, The School of Pharmacy, University of London, Brunswick Square, London, W.C.*1, *England*

Sand in the size ranges 18–20 mesh, 30–36 mesh and 44–60 mesh has been separated by means of a vibratory shape-sorting table into fractions of different shape. The ratios of the surface area of the particles to their volumes—the shape coefficients—ranged from 8 to 15. For each fraction the following properties were measured: angle of repose, bulk density and rate of flow through an orifice. In all cases, with increasing departure from the spherical, the angle of repose increased, whilst the bulk density and flowability decreased. Improved methods are reported for the measurement of bulk density, angle of repose and specific surface area in the range 30–130 cm^2/g.

It is generally accepted that the shape of the particles of a powder or a granular solid has an effect upon such bulk properties as angle of repose, bulk density and rate of flow through an orifice, but there is little published experimental work to support this intuitively acceptable statement. This arises from the difficulty of obtaining samples of a particular material which have the same particle size but different particle shapes and because of the labour involved in measuring the shape coefficients of the samples once they have been obtained. The shape coefficient used in the present work is the ratio of the surface area of a particle to its volume (see also p. 34 S).

The effect of particle shape on bulk properties, particularly orifice flow, has been given some attention by Fowler & Glastonbury (1959), Fowler & Chodziesner (1959) and by Pilpel (1965). Variation of particle shape was achieved only by using materials as different as wheat, rice, sugar and sand. The shape range covered was relatively narrow, and the density and surface structure were extremely diverse. The angle of repose was said to depend upon particle shape, particle density and the roughness of the supporting surface.

Working with lactose and starch granules, Fonner, Banker & Swarbrick (1966) obtained a shape variation by using different granulation methods. These authors found no dependence of angle of repose upon particle shape, but again, the particles differed not only in density, due to varying amounts of entrapped air, but also in surface structure.

In the present work, closely-sized batches of sand have been separated into fractions of different shape by using a vibratory shape-sorting table of a type originally developed for the shape classification of grinding grit in the diamond industry. The surface shape coefficient and volume shape coefficient as defined on p. 4 have been determined for the various fractions; the ratio of these two parameters, the shape coefficient, is the accepted criterion for the degree of departure of particle shape from the spherical. Angles of repose have been determined by two methods in which the base of the heap is formed by a static layer of the powder itself and the

angle is measured by weighing; bulk density, orifice flow rate and specific surface have also been measured. The aim of the work is to show that for any particlar material, these properties are a single-valued function of shape, so that a measurement of any of them will serve to characterise the particle shape of a new batch. Also, the rate of flow on a chute and the rate of mixing under the same conditions are being examined using the inclined plane apparatus described last year (Ridgway & Rupp, 1968) to see whether the effective diffusion coefficient between two flowing layers is also a function of particle shape.

EXPERIMENTAL

The material used was sand from King's Lynn, Norfolk and Leighton Buzzard, Herts. (supplied by British Industrial Sand Ltd., Reigate, and George Garside (Sand) Ltd., Leighton Buzzard). The sand was washed with water and dried in an air oven before being sieved into the required narrow size ranges. Particles with shape coefficients greater than 12 were scarce in these samples and to obtain more angular fractions some sand was mechanically crushed: this is a standard procedure for angular foundry sand manufacture. The required shape factor was obtained by the creation of flats and sharp angles rather than by the formation of particles whose principal axes were of different lengths, but no properties other than shape were affected by the crushing process.

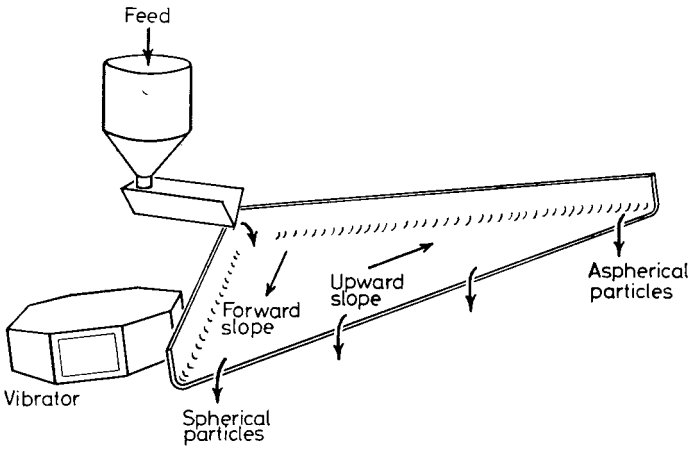

FIG. 1. The shape sorting table.

The shape-sorting table is shown diagrammatically in Fig. 1. It consists of a triangular metal deck carried on a tubular metal framework fitted with two screw-jacks so that the slope of the deck can be adjusted in two independent directions. The powder is fed onto the deck at one corner and moves across to the opposite side, fanning out as it goes. The vibration tends to make all particles ride up the slope across which they are travelling. The extent to which they ride up is governed by their area of contact with the deck and their inability to roll. The result is that near-spherical particles leave the deck at the lowest point of the exit edge, whilst block or flaky material leaves at the highest point of the same edge. The different

shape fractions are collected along this edge of the deck. Experimentation is necessary to find the best combination of table feed angles, table slope and vibration amplitude for optimum separation. The apparatus was originally developed for the sorting of industrial diamonds and is manufactured by Jeffrey-Galion Ltd., Johannesburg.

Bulk density

A 100 ml beaker with a known total capacity was filled under constant conditions. To do this, a funnel with a spout diameter of 0·8 cm was held centrally 2 cm above the top of the beaker. Sand was poured into the funnel so that the outlet ran full, and a 20% excess of sand was poured over and above the amount required to fill the beaker. Taking care not to shake the beaker, the sand was struck off level with a knife edge. Beaker and contents were then weighed, and the loose bulk density calculated. The reproducibility of this method was $\pm$ 0·15%, probably because no volumetric measurements of sand in a graduated cylinder is involved.

Angle of repose

Two methods of measuring the angle of repose were used; in one a heap of material was formed, and in the other a drained crater. In both methods, however, the actual angle was not measured except as a check: the apparatus was so arranged that the weight of powder standing on a defined base could be obtained. Using the known value of the bulk density, the volume of material could be found, and hence the cone angle required to give a heap having this volume.

Method (a): convex angle of repose. The apparatus is shown in Fig. 2A. The bottle, containing about 20% excess sand over that needed to make the heap, is inverted onto the upper plate. Sand flows through the orifice onto the lower plate, where it forms a heap. The heap is weighed and the angle of repose calculated.

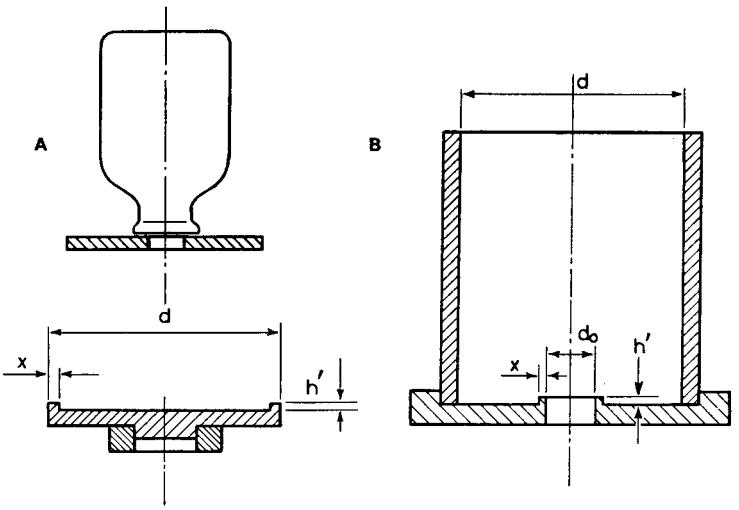

FIG. 2A. The apparatus for measuring the cone angle of repose.

FIG. 2B. The apparatus for measuring the crater angle of repose.

The volume, V, of a conical heap, height h and diameter d, is $\pi/12\ d^2h$. For a bulk density ρB and a heap weight w,

$$V = \frac{w}{\rho_B} \qquad \text{so that } h = \frac{12}{\pi} \cdot \frac{w}{\rho_B\, d^2}$$

and the angle of repose, α, is given by

$$\tan \alpha = \frac{2h}{d} = \frac{24}{\pi} \cdot \frac{w}{\rho_B\, d^3}$$

Successive determinations of α did not disagree by more than 0·1°, provided a plate having a ridge round the edge was used in order to make a defined base for the heap. Under such conditions the formula must be corrected to allow for the base layer of the heap. For the apparatus used here, the weight of the lower layer is given by

$$w' = \frac{\pi}{4}(d - 2x)^2\, h'\, \rho_B = 11{\cdot}55\, \rho_B$$

where x is the width and h′ the height of the ridge at the edge of the plate. Thus,

$$\tan \alpha = \frac{24}{\pi} \cdot \frac{w - 11{\cdot}55\, \rho_B}{\rho_B\, d^3}$$

Method (b): concave or crater angle of repose. This apparatus is shown in Fig. 2B. In use, it is filled with sand in the same manner as in the determination of bulk density. The bottom closure is then removed and the crater allowed to form. The weight of sand remaining in the container is then measured.

For this case,

$$V = \frac{w}{\rho_B} = \frac{\pi}{12} h(2d^2 - d_o^2 - d\, d_o)$$

$$\tan \alpha = \frac{2h}{d - d_o}$$

$$= \frac{24}{\pi} \cdot \frac{w}{(2d^2 - d_o^2 - dd_o)(d - d_o)\, \rho_B}$$

$$= \frac{24}{\pi} \cdot \frac{w}{(2d^3 - 3d^2\, d_o + d^3{}_o)\, \rho_B}$$

Some experiments were done to determine the effect of the size of the hole, d_o, and the height h′ of the ridge round the edge of it. For values of d_o less than eight particle diameters (0·95 cm), the angle of repose obtained is higher than with other methods. The height h′ had no effect over the range 0·075 to 0·32 cm.

Correction of the above formula due to the base layer of powder leads to the replacement of w by w − w′ where

$$w' = \frac{\pi}{4} h' (d^2 - d_o^2 - 4\, d_o x - 4x^2)\, \rho_B$$

Flowrate from an orifice

A vertical glass tube, 50 cm long and 2·5 cm internal diameter, had a flange coupling at the lower end to which could be attached one of a range of orifice plates. These

were made of thick brass sheet with the holes drilled and reamed to an accurate size and circularity. 200 g of the sand was poured carefully into the tube, and the orifice opened. Avoiding any measurement in the first or the last few centimetres of travel, the rate of flow was determined by timing with a stopwatch and weighing the quantity emerging.

The determination of the shape coefficient

For an arbitrarily-shaped particle with projected mean diameter d_a, two parameters are normally quoted, namely the surface and volume shape coefficients. Following the nomenclature of Heywood (1969), the definitions of these are that the surface area of the particle is

$$S = \alpha_{s,a} \cdot d_a^2$$

and its volume is

$$V = \alpha_{v,a} \cdot d_a^3$$

For a sphere, $\alpha_{s,a} = \pi$ and $\alpha_{v,a} = \pi/6$

The shape coefficient (without qualifying adjective) is the ratio of the above two quantities, i.e.

$$\alpha_{sv,a} = \alpha_{s,a}/\alpha_{v,a}$$

which has a numerical value of 6 for a sphere and increases as the particle shape departs from the spherical.

To determine the shape coefficient for a batch of particles, it is necessary to measure the average values of the particle volume, surface area and projected diameter.

Particle volume was determined by direct counting of a fairly large sample (between 300 and 800 particles, depending on mesh size). The counted sample was weighed and the average particle volume obtained by dividing by the true density of the sand, 2·65 g/cm^3.

The projected diameter d_a is the diameter of a circle having the same area as the projection of a particle resting in its most stable position. The mean projected diameter was measured by photographing a sample of particles under a low powered microscope. Prints were made on which individual particles had a diameter of at least 1·5 cm. About 100 particle pictures were cut out from the photograph and weighed: this gave the projected area of the 100 particles, and hence the mean projected diameter.

The surface area of the sand was more difficult to measure. In the range 30–130 cm^2/g air permeability is the only method. At measurable pressure drops across beds of sand however, the volume flowrate of air is large. Accordingly, a modified Lea and Nurse apparatus was constructed which had a much greater bed depth than normal. The sand was contained in a glass tube, 2·5 cm in diameter thus giving a bed depth of from 24 to 30 cm using a sample weight of 200 g. The bed depth was determined by inserting a flat-ended cylindrical rod. The length of the capillary resistance was reduced from 200 to 5 cm so that flowrates of up to 600 cm^3/min could be measured. The beds were packed by means of a vibrating tool and, for any one sample, measurements were made for at least two porosities and two flowrates. Fourfold variation of the flowrate caused no consistent trend in the surface area results obtained, and overall reproducibility was usually within 1%, with occasional readings at $\pm$ 2%.

RESULTS AND DISCUSSION

The properties of the various sand fractions which were prepared are given in Table 1, where the bulk density is also listed. Fig. 3 shows the trend of bulk density with shape coefficient. For all size ranges, the bulk density falls as the shape of the particles becomes less regular.

Table 1. *Shape coefficient, specific surface area and bulk density of the material used*

Sample and mesh size	Sand*	Projected diameter (cm)	Volume coefficient $\alpha_{v,a}$	Surface coefficient $\alpha_{s,a}$	Shape coefficient $\alpha_{sv,a}$	Specific surface area (cm^2/g)	Bulk density (g/cm^3)
44/60–1	n	0·0343	0·345	3·03	8·78	97·2	1·443
–2	n	0·0357	0·256	2·68	10·47	110·4	1·375
–3	c	0·0386	0·270	2·91	10·77	105·5	1·341
–4	n	0·0358	0·271	2·99	11·03	116·3	1·348
–5	c	0·0423	0·209	2·57	12·30	109·5	1·294
–6	n	0·0378	0·198	2·58	13·03	130·5	1·270
–7	c	0·0451	0·179	2·47	13·80	115·3	1·235
30/36–1	n	0·0559	0·428	3·28	7·66	51·5	1·528
–2	n	0·0609	0·375	2·89	8·70	54·1	1·488
–3	n	0·0661	0·302	2·98	9·81	56·4	1·442
–4	n	0·0694	0·246	2·84	11·54	62·8	1·386
–5	c	0·0755	0·208	3·07	14·76	73·8	1·231
18/20–1	n	0·0909	0·433	3·54	8·17	34·0	1·552
–2	n	0·0967	0·368	3·39	9·21	36·0	1·504
–3	n	0·1024	0·318	3·14	9·87	36·5	1·486
–4	n	0·1051	0·279	3·08	11·04	39·5	1·436
–5	c	0·1128	0·187	2·82	15·08	50·6	1·286

* n = natural
c = crushed

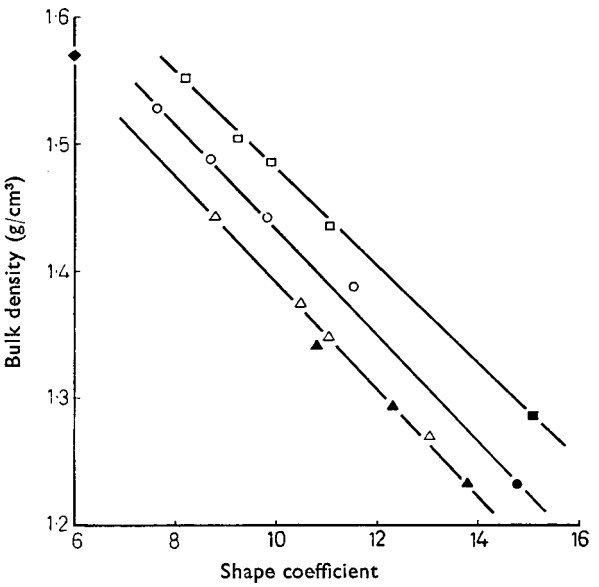

FIG. 3. Bulk density as a function of shape factor for three different sizes of sand. The following point convention applies to all graphs: open points: □ mean projected diameter 805 μm, ○ mean projected diameter 461 μm, △ mean projected diameter 302 μm; closed points, ■, ● and ▲ refer to crushed sand of the same mean diameters.

The point on the bulk density axis at 1·57 g/cm³ is the experimentally determined density for spheres of true density 2·65 g/cm³ formed into a loose-packed random array. All three lines should converge at this point, since for spherical particles, bulk density is not a function of absolute size, provided the container is large. In practice this is not the case, and the larger particles give the larger bulk densities, presumably because the impact energy as they are deposited into the container is greater. Macrae & Gray (1961) have shown that increased energy of deposition gives higher bulk density in sphere packings. Although quite a good linear relation applies between bulk density and shape factor, the linearity cannot extend much beyond the range covered by the graph. The bulk density cannot be expected to decline toward zero at a linear rate as the particles become more flaky: the bulk density extrapolates to zero at a shape factor of 45 on the graph shown.

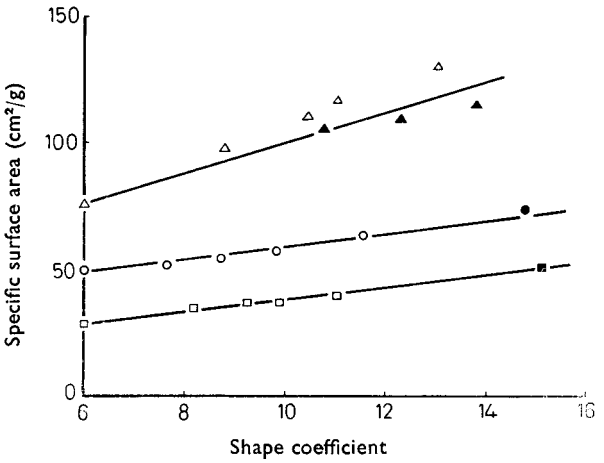

FIG. 4. Specific surface area as a function of shape factor.

Fig. 4 shows the relation between specific surface area and shape factor at constant particle size. Here also the points on the vertical axis are the calculated surface areas for spherical particles of the mean size of each of the sand fractions used. These values are listed in Table 2. Both crushed and natural sand fractions lie close to the same line. That for crushed sand there are three points lying slightly below the line for the smallest particles, is due to the differing size distributions within the fractions.

Table 2. *The mean diameters of the sand fractions used, and the properties of the equivalent sphere*

Mesh size	Size μm	Mean diameter μm	Wt. of one sphere, g	Particles per g	Surface area of one sphere, cm²	Specific surface cm²/g
18–20	853–758	805	$7{\cdot}2 \times 10^{-4}$	$1{\cdot}4 \times 10^{3}$	$2{\cdot}03 \times 10^{-2}$	28·2
30–36	500–422	461	$1{\cdot}35 \times 10^{-4}$	$7{\cdot}4 \times 10^{3}$	$6{\cdot}7 \times 10^{-3}$	49·3
44–60	353–251	302	$3{\cdot}8 \times 10^{-5}$	$2{\cdot}6 \times 10^{4}$	$2{\cdot}9 \times 10^{-3}$	75·5

The 44–60 mesh crushed sand was the extreme fines, sieved out from a coarse batch of which only about 1% was in fact below 44 mesh size. Thus within this

fraction, 60 mesh particles will be scarce. The 44–60 mesh natural sand was sieved from a batch ranging from 30 to 150 mesh, so that 44 and 60 mesh particles are present in more nearly equal proportions. The true mean size of the crushed sand fractions is probably larger than the mean sieve aperture.

As a check on the modified air permeability method, surface areas were measured on three samples of glass ballotini. These compare well with the calculated values (Table 3). Ideally it would have been preferable to measure the surface area for spheres having the diameters of Table 2 but these were not available.

Table 3. *Experimental and calculated surface areas for spherical particles using the modified air permeability apparatus*

Mean particle size μm	Porosity	Specific surface area, cm²/g	
		experimental	calculated
350	0·336	56·0	56·7
350	0·321	57·8	56·7
275	0·336	67·8	73·9
275	0·325	67·3	73·9
195	0·334	97·2	104·2
195	0·309	97·0	104·2

Table 4. *Angle of repose and orifice flow in relation to particle size shape*

Sample and mesh size	Shape coefficient $\alpha_{sv,a}$	Angle of repose in degrees		Orifice flow (g/s)			
				Orifice diameter (cm)			
		Concave	Convex	0·953	0·793	0·634	0·476
44/60–1	8·78	35·21	35·1	18·93	11·28	6·41	2·75
–2	10·47	36·6	36·9	18·28	11·14	6·01	2·56
–3	10·77	37·0	36·7	17·73	11·59	6·11	2·58
–4	11·03	37·4	37·5	18·14	11·00	5·78	2·49
–5	12·03	38·3	38·3	17·60	11·06	5·77	2·44
–6	13·03	38·6	38·7	17·87	9·94	5·33	2·30
–7	13·80	39·8	39·6	17·19	9·83	5·32	2·20
30/36–1	7·66	35·3	35·2	18·46	10·49	5·65	2·34
–2	8·70	37·4	37·2	18·11	10·38	5·47	2·24
–3	9·81	39·3	38·8	17·96	10·24	5·28	2·14
–4	11·54	40·6	40·5	17·30	9·69	4·96	2·01
–5	14·76	43·0	42·1	13·85	8·24	4·32	1·63
18/20–1	8·17	37·9	36·8	15·85	8·70	4·48	—
–2	9·21	40·5	39·2	15·44	8·44	4·31	—
–3	9·87	41·6	40·8	15·15	8·24	4·13	—
–4	11·04	43·2	42·1	14·63	7·91	3·98	—
–5	15·08	45·6	43·1	12·23	7·06	3·54	—

Table 4 lists the experimental results for angle of repose and for flowrate through a range of orifices. Fig. 5 shows the measured angles of repose as a function of the shape coefficient. The point on the vertical axis is the angle of repose as determined by the two methods for ballotini of each of two sizes. All four measured angles agreed to 0·15°, the mean being 27·4°. Thus for spheres and for the smaller sand particles, the two methods give results which do not differ, but the influence of shape in giving a difference between the two methods is very apparent for the larger particles. The crater method is the better to use as a test of particle shape, since the rate of change of angle with shape is greater, especially at the higher shape coefficients.

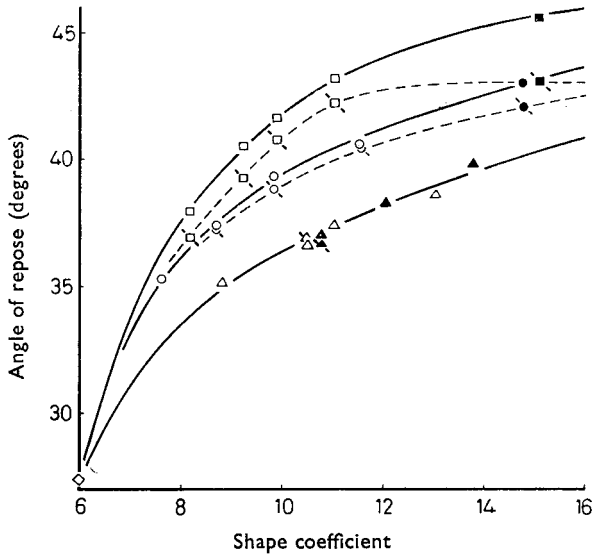

FIG. 5. Angle of repose as a function of shape coefficient for three sizes of sand. The point on the vertical axis is the angle of repose measured for glass ballotini by both methods. Points with a diagonal line, represent the convex heap method; normal points refer to the crater method.

In all cases (Fig. 6), an increase in shape factor leads to a decrease in flowrate through an orifice. This is in line with the angle of repose measurements in that the resistance to shear, or flow, of an assembly of irregular particles is greater than that of an assembly of spherical particles of the same size and density.

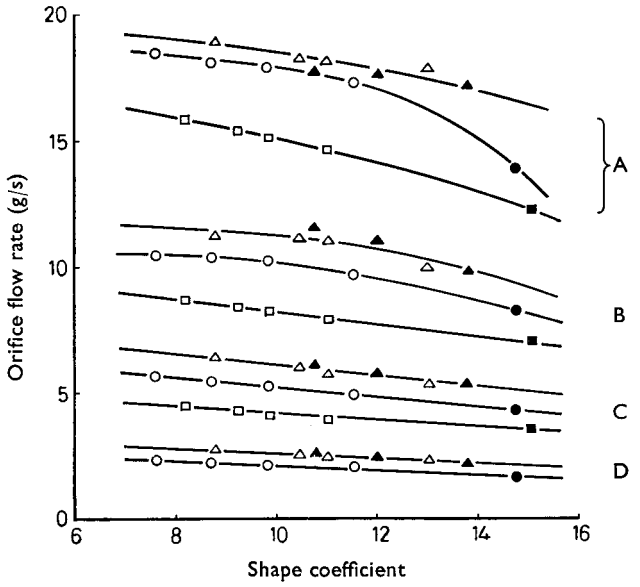

FIG. 6. Efflux rate from an orifice as a function of particle shape. Orifice diameter—A, 0·953 cm; B, 0·793 cm; C, 0·634 cm; D, 0·476 cm.

REFERENCES

FONNER, D. E., BANKER, G. S. & SWARBRICK, J. (1966). *J. pharm. Sci.*, **55**, 181.

FOWLER, R. T. & CHODZIESNER, W. B. (1959). *Chem. Engng Sci.*, **10**, 157–162.

FOWLER, R. T. & GLASTONBURY, J. R. (1959). *Ibid.*, **10**, 150–156.

HEYWOOD, H. (1969). Paper delivered at Inst. Chem. Engrs Symposium "Powder Research", London, March 5th, 1969.

MACRAE, J. C. & GRAY, W. A. (1961). *J. appl. Phys.*, **121**, 164.

PILPEL, N. (1965). *Chem. Proc. Engng*, 167–171.

RIDGWAY, K. & RUPP, R. (1968). *J. Pharm. Pharmac.*, **19**, *Suppl.*, 185S–193S.